ELSEVIER

Thin Solid Films 270 (1995) 555–560

thin solid films

Silicide formation and stability of Ti/SiGe and Co/SiGe

Zhihai Wang, D.B. Aldrich, Y.L. Chen, D.E. Sayers, R.J. Nemanich

Department of Physics, North Carolina State University, Raleigh, NC 27695-8202, USA

Abstract

The formation and stability of the products of Ti and Co reacting with $Si_{1-x}Ge_x$ substrates were investigated. For the Ti/SiGe system, when a C54 $Ti(Si_{1-y}Ge_y)_2$ layer forms, the Ge index y is initially the same as the Ge index of the $Si_{1-x}Ge_x$ substrate (i.e. $y=x$). Thereafter $Si_{1-x}Ge_x$ from the substrate continues to diffuse into the C54 layer via lattice and grain-boundary diffusion. Some of the Si which diffuses into the C54 lattice replaces Ge in the lattice, and the C54 $Ti(Si_{1-y}Ge_y)_2$ becomes silicon enriched (i.e. $y<x$). For the Co/SiGe system, it was determined that a silicon-enriched $Co(Si_{1-y}Ge_y)$ layer was formed at ~400 °C. As the annealing temperature was increased, the reacted layer became even more Si enriched. For both materials systems, Ge-enriched $Si_{1-z}Ge_z$ ($z>x$) islands were observed. It was found that for $Co/Si_{1-x}Ge_x$ the reacted layer consisted of $CoSi_2$ and $Si_{1-z}Ge_z$ after high-temperature annealing (≈700 °C). We propose that these processes are driven by a reduction in the crystal energy of the C54 $Ti(Si_{1-y}Ge_y)_2$ phase in the Ti/SiGe system and the $Co(Si_{1-y}Ge_y)$ phase in the Co/SiGe system which accompanies the replacement of Ge with Si.

Keywords: Silicides; Titanium; Cobalt; Annealing

1. Introduction

Epitaxial $Si_{1-x}Ge_x$ alloys on Si(100) are of interest because of their potential device applications. Recently, advanced devices have been demonstrated based on $Si_{1-x}Ge_x/Si$ heterojunctions [1–4]. In device applications, it may be necessary to make Schottky or Ohmic contacts with the epitaxial $Si_{1-x}Ge_x$ alloys. Metal silicides are important candidates for such contacts. Knowledge about reactions between thin metal films and epitaxial $Si_{1-x}Ge_x$ is essential for applications with $Si_{1-x}Ge_x$ devices. Recently, significant effort has been made to study the phase formation of metal/$Si_{1-x}Ge_x$ reactions and the properties of reacted materials [5–20]. Currently the C54 phase of titanium disilicide ($TiSi_2$) is used in microelectronics for interconnects and source and drain contacts. Also, $CoSi_2$ is being considered as an alternate to $TiSi_2$ for these applications because of several advantages of $CoSi_2$, such as its expitaxial nature with Si and stability in the presence of dopants. The C54 phase of $TiSi_2$ and $CoSi_2$ have similar low resistivities (~15 μΩ cm) [21]. The importance of $TiSi_2$ and $CoSi_2$ in Si-based devices and the increasing use of $Si_{1-x}Ge_x$ motivates the investigation of the metallization of Ti or Co on $Si_{1-x}Ge_x$ alloys [11–20].

The bilayer solid-phase Ti–Si and Ti–Ge reactions usually result in the formation of at least two prominent phases in each reaction. The two phases observed in the Ti–Si reaction are C49 $TiSi_2$ (base-centered orthorhombic [22]) and C54 $TiSi_2$ (face-centered orthorhombic [22]). The two phases formed in the Ti–Ge solid phase reaction are Ti_6Ge_5 and C54 $TiGe_2$ (isomorphic with C54 $TiSi_2$) [23,24]. There is no analogy in the Ti–Si system for Ti_6Ge_5 and likewise C49 $TiGe_2$ has not been observed in the Ti–Ge solid-phase reaction. It has been shown previously that C54 $Ti(Si_{1-y}Ge_y)_2$, isomorphic with C54 $TiSi_2$, results from the high-temperature solid-phase reaction of Ti and $Si_{1-x}Ge_x$ over the entire alloy composition range ($0.0<x<1.0$) [11,12,25].

The cobalt silicide phases, Co_2Si, CoSi, and $CoSi_2$, form in sequence when a Co/Si bilayer structure is annealed [20,26,27]. The formation temperatures of CoSi and $CoSi_2$ are ~400 °C and ~550 °C, respectively. Previous studies found that the Co_5Ge_7 and $CoGe_2$ phases formed after annealing a Co/Ge bilayer structure at temperatures above 300 °C, with formation of Co_5Ge_7 at about 300 °C and $CoGe_2$ at about 600 °C [20,28]. According to the bulk ternary phase diagram of the Co–Si–Ge system, a miscible ternary compound $Co(Si_{1-x}Ge_x)$ ($x<0.67$) exists, which is based on cubic CoSi [29]. The crystal structures of $CoSi_2$ and $CoGe_2$ are different. $CoSi_2$ has a cubic CaF_2 structure while $CoGe_2$ has an orthorhombic structure[28].

In the present study of bilayer solid-phase reactions of Ti and Co with $Si_{1-x}Ge_x$ ($x=0.32$ for Ti and $x=0.20$ for Co), we have investigated phase formation and stability of the formed phases at various annealing temperatures. X-ray diffraction (XRD), energy dispersive X-ray spectroscopy

SSDI 0040-6090(95)06841-4

(EDXS), and Auger electron spectroscopy (AES) were used to examine the structural and compositional properties of the reacted thin films. The morphologies of surfaces and interfaces were examined using scanning electron microscopy (SEM) and cross-sectional transmission electron microscopy (XTEM).

2. Experiment

In this study, 25 mm diameter, n-type, Si(100) wafers with a resistivity of 0.8–1.2 Ω cm were used as substrates. Strained single-crystal $Si_{1-x}Ge_x$ ($x=0.20$ and 0.32) alloy thin films, 800 Å to 2500 Å thick, were epitaxially grown on atomically clean Si substrates at 550 °C in a custom-made molecular beam epitaxy (MBE) system (base pressure $<2\times10^{-10}$ Torr). The procedure for obtaining an atomically clean Si substrate has been described previously [25]. For Ti metallization, 400 Å of titanium was deposited from an in-situ hot-filament Ti source. Upon completion of the titanium deposition, the samples were annealed in-situ at temperatures of 530 °C, 570 °C, 660 °C, or 700 °C for 10 min. The $Si_{1-x}Ge_x$ thin film samples prepared for Co metallization were transferred from the MBE chamber. Prior to Co metallization, which was carried out in a separate UHV chamber with a base pressure $<3\times10^{-10}$ Torr using an electron beam evaporator, the $Si_{1-x}Ge_x$ sample was cleaned by the same procedure for cleaning the Si wafer except that the thermal desorption was performed at 700 °C. For each Co/SiGe sample, a 200 Å polycrystalline Co layer was deposited. The metallized sample was then annealed in-situ at 400 °C, 500 °C, 600 °C, or 700 °C for 20 min.

3. Results

3.1. $Ti/Si_{0.68}Ge_{0.32}$ solid-state reaction

XRD was used to determine the structure of the titanium germanosilicide films that formed from the 10 min annealing of the $Ti/Si_{0.68}Ge_{0.32}$ bilayer structures. The XRD scan of the sample annealed at 530 °C contained peaks corresponding to diffraction from the (150) and (200) planes of C49 $Ti(Si_{1-y}Ge_y)_2$. The XRD scans of the samples annealed at 570 °C, 660 °C, and 700 °C all contained peaks corresponding to diffraction from the (311), (004), (022), and (313) planes of C54 $Ti(Si_{1-y}Ge_y)_2$ (see Fig. 1). The diffraction peaks of the C54 phase found in the 570 °C, 660 °C, and 700 °C samples were observed to shift to higher angles with increasing annealing temperature, indicating changes in the spacing of the diffracting planes. The Ge indices of the C54 $Ti(Si_{1-y}Ge_y)_2$ in these samples were calculated by: (1) calculating the diffraction plane spacings using XRD, (2) calculating the C54 lattice parameters from the plane spacings, (3) calculating the volumes of the C54 unit cells, and (4) comparing the calculated unit cell volumes with the known

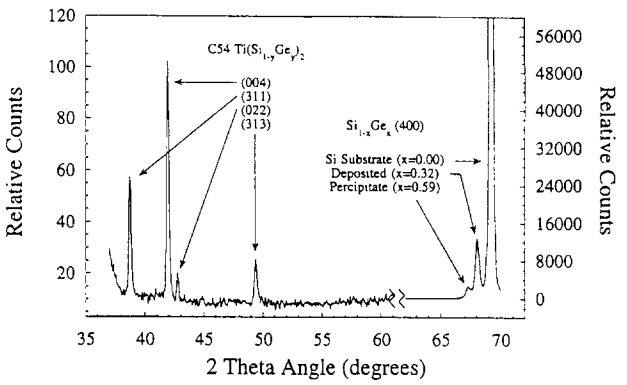

Fig. 1. X-ray diffraction scan of a $Ti/Si_{0.68}Ge_{0.32}$ bilayer structure which has been annealed for 10 min at 700 °C to form C54 $Ti(Si_{1-y}Ge_y)_2$.

unit cell volumes of C54 $TiSi_2$ and C54 $TiGe_2$. In a study by Boutarek and Madar [30], it was observed that the C54 $Ti(Si_{1-y}Ge_y)_2$ unit cell volume varies linearly with the Ge index y. In this study, the C54 composition determination was based on the C54 unit-cell volume (using all three lattice parameters instead of just a single lattice parameter) to reduce errors which would occur if the C54 unit cell was distorted by strain. The Ge indices of the C49 $Ti(Si_{1-y}Ge_y)_2$ formed at 530 °C and the C54 $Ti(Si_{1-y}Ge_y)_2$ formed at 570 °C, 660 °C and 700 °C are 0.31, 0.32, 0.28, and 0.24, respectively. These results indicate that the Ge indices of $Ti(Si_{1-y}Ge_y)_2$ in the samples annealed at 530 °C and 570 °C are approximately equal to the Ge index of the deposited $Si_{0.68}Ge_{0.32}$ alloy (i.e. $y=0.32$). At the higher annealing temperatures of 660 °C and 700 °C, the observed decrease in the Ge index indicates that Ge in the C54 $Ti(Si_{1-y}Ge_y)_2$ is being replaced by Si (i.e. $y<0.32$). The XRD scans of these samples included the range where the Si (400), Ge (400), and $Si_{1-x}Ge_x$ (400) diffraction peaks occur, as shown in Fig. 1. At 530 °C and 570 °C, the only XRD peaks observed in this range corresponded to the Si substrate and the remaining unreacted $Si_{0.68}Ge_{0.32}$ alloy layer. At 660 °C and 700 °C, in addition to the peak of the unreacted $Si_{0.68}Ge_{0.32}$, a peak corresponding to $Si_{0.41}Ge_{0.59}$ ($z=0.59\pm0.04$) was observed.

Scanning electron micrographs of the surface morphologies of the samples annealed at 660 °C and 700 °C are shown in Fig. 2. After annealing at 660 °C, the formation of decorations along the C54 grain boundaries was observed (Fig. 2(a)). An increase in the average size and areal density of the decorations was observed for the sample annealed at 700 °C (Fig. 2(b)). Grain boundary decorations were not observed in the samples annealed at 530 °C or 570 °C. The morphology, structure, and composition of the C54 grains and the grain boundary decorations of the 700 °C sample were more closely examined using XTEM, EDXS, and micro-diffraction. It was found that the decorations are Ge-rich $Si_{1-z}Ge_z$ alloy ($z>x$), where x is the Ge index of the $Si_{0.68}Ge_{0.32}$ alloy layer. It was also observed that the $Si_{1-z}Ge_z$ decorations extend from the sample surface to the underlying $Si_{0.68}Ge_{0.32}$ alloy layer, effectively separating the neighboring C54 $Ti(Si_{1-y}Ge_y)_2$ grains [31].

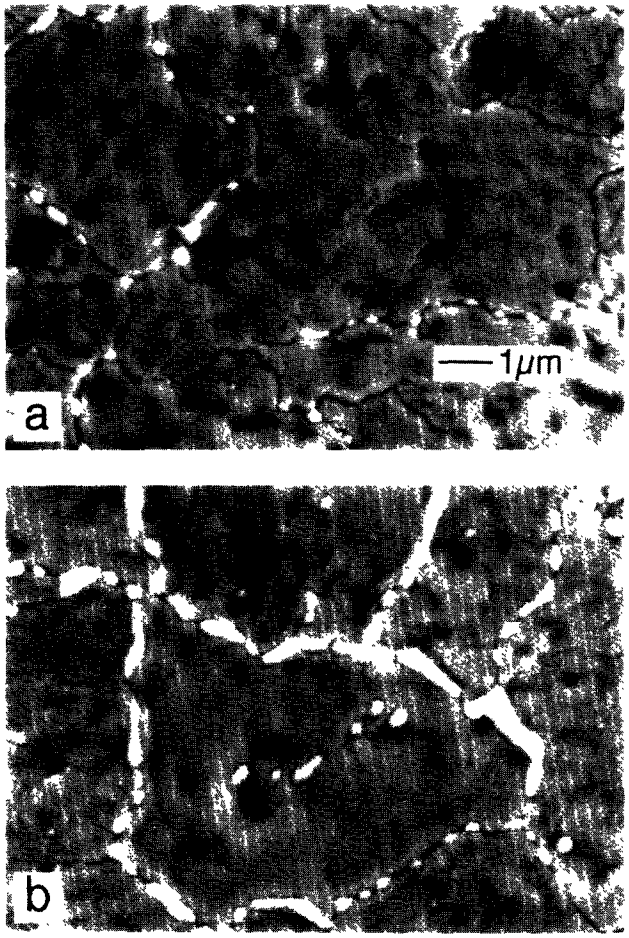

Fig. 2. SEM micrographs of the morphology of the $Ti/Si_{0.68}Ge_{0.32}$ samples annealed for 10 min at 660 °C and 700 °C. After annealing at 660 °C $Si_{1-z}Ge_z$ decorations are observed along the C54 $Ti(Si_{1-y}Ge_y)_2$ grain boundaries (a). After annealing at 700 °C the grain boundary decorations occupy a significant portion of the C54 grain boundaries (b).

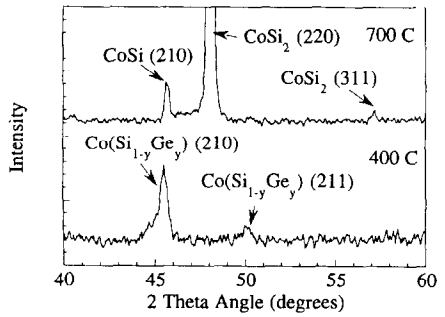

Fig. 3. X-ray diffraction scans of two $Co/Si_{0.80}Ge_{0.20}$ bilayer structures which have been annealed for 20 min at 400 °C and 700 °C, respectively.

3.2. *$Co/Si_{0.80}Ge_{0.20}$ solid-state reaction*

XRD scans of the samples annealed at 400 °C and 700 °C are shown in Fig. 3. For the 500 °C and 600 °C annealed samples, the diffraction patterns are similar to those of the 400 °C annealed sample. The two peaks shown in Fig. 3 for the 400 °C annealed sample can be associated with two diffracting planes of the cubic CoSi structure. This suggests that the reacted layers at these temperatures contain materials with the CoSi structure. However, the peak positions of peaks were located at angles lower than those of CoSi. This shift can be associated with an expansion of inter-plane spacing of the corresponding diffraction planes. Because homogenous solid solutions between CoSi and CoGe exist, the phase formed at these temperatures should be $Co(Si_{1-y}Ge_y)$, which has a larger lattice constant than CoSi, causing the observed peak shifts. By assuming that the lattice constant of $Co(Si_{1-y}Ge_y)$ is a linear interpolation of CoSi and CoGe, we calculated the Ge indices y of $Co(Si_{1-y}Ge_y)$. The calculated Ge indices are 0.12, 0.09 and 0.05 for the samples annealed at 400 °C, 500 °C, and 600 °C, respectively. These y values are considerably less than the Ge index in the underlying $Si_{0.80}Ge_{0.20}$ layer, and decrease with increasing annealing temperature. For the 700 °C annealed sample, peaks associated with $CoSi_2$ and a weak peak associated with the (210) diffraction of CoSi were observed in the X-ray diffraction scan. No Co–Ge phase was observed. These results indicate that at this temperature Ge had nearly completely segregated out from the $Co(Si_{1-y}Ge_y)$ phase. A broad peak associated with the (400) plane of $Si_{0.50}Ge_{0.50}$ was also identified in this sample.

A scanning electron micrograph of the surface morphology of the sample annealed at 500 °C is shown in Fig. 4. "Flower-shaped" features were observed. The sample annealed at 400 °C had the same surface morphology but the contrast between the flower-shaped features and the surrounding smooth area is less pronounced than that of the 500 °C annealed sample. Scanning micro-probe AES was used to determine the element compositions on the surface of these flower-shaped features and the surrounding smooth area. It was found that these flower-shaped features were Ge-enriched clusters, and the Ge composition increased with increasing annealing temperature. Whether these Ge-rich clusters are $Si_{1-z}Ge_z$ ($z > x$) is not clear at present because Co Auger signals were also detected when probing the cluster area. But these Co signals may originate from the open area (i.e. the area not covered by the cluster) nearby or under the cluster. It was also found that the Ge composition is uniform over the smooth surface area. AFM was used to examine the surface roughness of

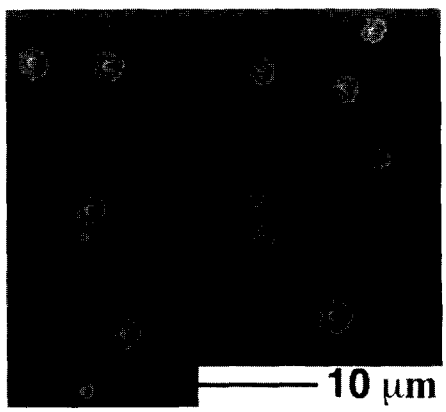

Fig. 4. SEM micrograph of the morphology of the 500 °C annealed $Co/Si_{0.80}Ge_{0.20}$ sample. The "flower-shaped" features appear on smooth surfaces. Micro-probe AES analysis reveals that these features are Ge-enriched clusters.

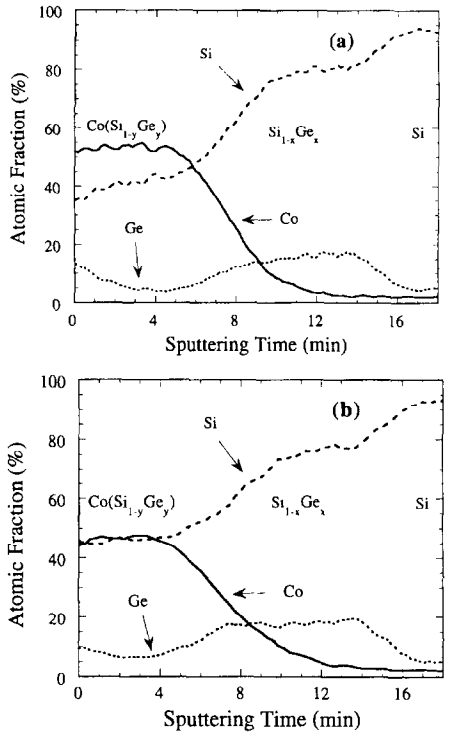

Fig. 5. Micro-probe Auger depth profiles of (a) the 400 °C annealed and (b) the 500 °C annealed $Co/Si_{0.80}Ge_{0.20}$ samples. The electron beam was focused on a spot on the smooth surface area.

these samples. It was found that the Ge-rich clusters extended above the surrounding smooth surface. XTEM examination of one of these Ge-rich clusters showed that while most of the cluster resided on top of the $Co(Si_{1-y}Ge_y)$ layer, part of the cluster was embedded into the grain boundaries of the $Co(Si_{1-y}Ge_y)$ layer. The results of micro-probe AES depth profiles on the smooth area of the 400 °C and 500 °C samples are shown in Fig. 5. As indicated, Co was uniformly distributed in the reacted layer while some Co had diffused into the underlying $Si_{0.80}Ge_{0.20}$ layer. In the reacted layer, Si and Ge were not uniformly distributed. For the 400 °C annealed sample, the Ge composition was highest at the sample surface and decreased gradually into the reacted layer (Fig. 5(a)). For this sample, it can also be found from the Auger data shown in Fig. 5(a) that the relative atomic ratio of Ge over Si in the surface layer is higher than that of the underlying $Si_{0.80}Ge_{0.20}$ layer, and the same relative ratio in the middle of the reacted layer was less than that of the underlying $Si_{0.80}Ge_{0.20}$ layer. A detailed analysis showed that the Ge/Si atomic ratio at the sample surface was about four times higher than that of the underlying $Si_{0.80}Ge_{0.20}$ layer, and the same ratio in the middle of the reacted layer was less than one-third of that of the underlying $Si_{0.80}Ge_{0.20}$ layer. For the 500 °C annealed sample, although the Ge composition was still higher in the near-surface region than that in the middle of the reacted layer, the relative atomic ratio of Ge over Si Ge/Si atomic ratio in the entire reacted layer was below that of the underlying $Si_{0.80}Ge_{0.20}$ layer. The broadened XRD peak of the 400 °C annealed sample (see Fig. 3) is consistent with the non-uniform distribution of Ge atoms in the reacted layer.

These results indicate that the Ge index in the $Co(Si_{1-y}Ge_y)$ layer obtained by XRD can only be considered to be an average Ge composition in the entire reacted layer. The fact that the decrease of the Ge index in the $Co(Si_{1-y}Ge_y)$ layer was accompanied by an increase of Ge content in the flower-shape clusters when the annealing temperature was increased implies that Ge inside the $Co(Si_{1-y}Ge_y)$ lattice was replaced by Si, and excess Ge diffused to the grain boundaries and the surface to form the Ge-enriched clusters. AFM was also used to examine the surface roughness of these samples. It was found that the Ge-rich clusters extended above the surrounding smooth surface.

4. Discussion

It was observed that the $Ti(Si_{1-y}Ge_y)_2$ and $Co(Si_{1-y}Ge_y)$ phases were not stable when in contact with the $Si_{1-x}Ge_x$ alloy. The results indicated that germanium segregated out of these germanosilicide phases (replaced by silicon available from the substrate) effectively changing the composition of the germanosilicide. In the Ti–$Si_{1-x}Ge_x$ system, the measured compositions indicate that the $Ti + Si_{1-x}Ge_x \rightarrow$ C54 $Ti(Si_{1-y}Ge_y)_2 + Si_{1-z}Ge_z$ ($y < x < z$) reaction can be separated into a two-step process: (1) C54 formation and (2) germanium segregation (Eqs. (1) and (2), respectively).

$$Ti + Si_{1-x}Ge_x \Rightarrow C54\ Ti(Si_{1-x}Ge_x)_2 \quad (1)$$

$$C54\ Ti(Si_{1-x}Ge_x)_2 + Si_{1-x}Ge_x \rightarrow C54\ Ti(Si_{1-y}Ge_y)_2 + Si_{1-z}Ge_z (y < x < z) \quad (2)$$

Our results indicate that at the C54 formation temperature the C54 $Ti(Si_{1-y}Ge_y)_2$ forms with the same Ge index as the deposited $Si_{1-x}Ge_x$ layer (i.e. $y = x$). As the annealing temperature is increased, Ge on the C54 lattice is replaced by Si and the Ge index of the C54 $Ti(Si_{1-y}Ge_y)_2$ decreases ($y < x$). The decrease in the Ge index of the C54 titanium germanosilicide occurs concurrently with the observed formation of Ge-rich $Si_{1-z}Ge_z$ alloy grain boundary decorations ($z > x$). Excess Ge which diffuses to the C54 grain boundaries combines with Si and Ge from the substrate and nucleates as Ge-rich $Si_{1-z}Ge_z$ ($z > x$). The nucleation of $Si_{1-z}Ge_z$ at the C54 grain boundaries establishes a sink for excess Ge and enables the replacement of Ge with Si on the C54 lattice to continue.

With the $Co/Si_{1-x}Ge_x$ system, an intermediate ternary phase, i.e. $Co(Si_{1-y}Ge_y)$, was formed at annealing temperatures from 400 °C up to 600 °C. The Ge index in this ternary phase was lower than that of the underlying $Si_{0.80}Ge_{0.20}$ alloy layer and decreased with increasing annealing temperature. The distribution of Ge was not uniform in the reacted layer with the top part of the reacted layer being relatively rich in Ge. The temperature dependence of the Ge composition suggests that Ge inside the $Co(Si_{1-y}Ge_y)$ lattice was replaced by Si during the annealing. The Ge atoms segregated out from the ternary compound and diffused to the sample surface

and formed Ge-enriched clusters through grain boundary and surface diffusion.

A possible driving force for the segregation of Ge from the C54 $Ti(Si_{1-y}Ge_y)_2$ and $Co(Si_{1-y}Ge_y)$ lattices can be found in the relative crystal energies between the C54 $TiSi_2$ and C54 $TiGe_2$ structures and between the CoSi and CoGe structures. As a first-order approximation, the heat of formation of these materials can be used as an approximation of the relative crystal energies of these materials. We further assume that the heat of formation (i.e. crystal energy) of a ternary compound is a linear interpolation between the heat of formation values of its two end-point binary compounds (another first order approximation). Under these approximations, the crystal energies of $Ti(Si_{1-y}Ge_y)_2$ and $Co(Si_{1-y}Ge_y)$ alloys will be lowered if Ge atoms are replaced by Si atoms in both structures because the heats of formation of the silicides ($TiSi_2$ and CoSi) are lower than the germanides ($TiGe_2$ and CoGe). From thermodynamic data, the heats of formation are -57.0, -47.5, -100.4, and -34.2 kJ mol^{-1} for $TiSi_2$, $TiGe_2$, CoSi, and CoGe, respectively [30]. This suggests that the crystal energy will drop if the Ge atoms are replaced by Si atoms in both structures. Using these data, the amount of crystal energy reduction, ΔG, by replacing Ge with Si in these two structures can be calculated using the following equation:

$$\begin{aligned} \Delta G &= -(9.5\text{kJ mol}^{-1})\,\delta y \quad \text{for } Ti(Si_{1-y}Ge_y)_2 \\ \Delta G &= -(66.2\text{kJ mol}^{-1})\,\delta y \quad \text{for } Co(Si_{1-y}Ge_y) \end{aligned} \tag{3}$$

where δy is the change in Ge index in the C54 $Ti(Si_{1-y}Ge_y)_2$ or $Co(Si_{1-y}Ge_y)$ structure. Eq. (3) was obtained using an approximation which states that the heat of formation (i.e. crystal energy) of a ternary compound is a linear interpolation between the heat of formation values of its two end-point binary compounds. From this analysis, it can be expected that the Ge segregation in the $Co(Si_{1-y}Ge_y)/Si_{1-x}Ge_x$ system would be more severe than in the $Ti(Si_{1-y}Ge_y)_2/Si_{1-x}Ge_x$ system. Our results support this supposition. We suggest that the diffusivities of silicon and germanium in these structures, which are not available at present, will effect the speed of the segregation, but will not alter the general tendency of the segregation. The above discussion may be extended to other metal/SiGe systems to estimate the stability of the metal–SiGe compounds in those systems formed by solid-state reaction.

It is interesting to compare the formation temperature of $CoSi_2$ in the Co/Si binary system with that in the $Co/Si_{1-x}Ge_x$ system. The formation temperature of $CoSi_2$ is around 550 °C in the Co/Si system. But in the $Co/Si_{1-x}Ge_x$ system, $CoSi_2$, together with some residual CoSi, was only observed at higher temperatures (700 °C) as shown in Fig. 3. At this temperature, Ge was totally separated from the formed Co–Si phases, and no Co–Ge phase was observed. These observations suggest that $CoSi_2$ nucleated after all Ge atoms were segregated out from the $Co(Si_{1-y}Ge_y)$. It is worth pointing out that the heat of formation of $CoSi_2$ (-102.9 kJ mol^{-1}) is significantly lower than that of $CoGe_2$ (-17.4 kJ mol^{-1}). [32] This may explain why $CoGe_2$ was not observed in the 700 °C annealed sample.

5. Conclusion

The formation and stability of C54 $Ti(Si_{1-x}Ge_x)_2$ and $Co(Si_{1-y}Ge_ySiGe)$ produced from the solid-phase reaction of Ti and Co with $Si_{1-x}Ge_x$ have been investigated. For the Ti/SiGe system, the reaction can be separated into two stages:

$$\text{Ti} + Si_{1-x}Ge_x \rightarrow \text{C54 } Ti(Si_{1-x}Ge_x)_2$$

and (4)

$$\text{C54 } Ti(Si_{1-x}Ge_x)_2 + Si_{1-x}Ge_x \rightarrow \text{C54 } Ti(Si_{1-y}Ge_y)_2 + Si_{1-z}Ge_z$$

where $y < x < z$. For the Co/SiGe system, a $Co(Si_{1-y}Ge_y)$ layer with $y \approx 0.12$ was initially formed. It was found that the Ge indices in the C54 $Ti(Si_{1-y}Ge_y)_2$ and $Co(Si_{1-y}Ge_y)$ decreased with increasing annealing temperature. A thermodynamic driving force is used to explain these results. The replacement of Ge with Si in titanium and cobalt germanosilicide causes a reduction of the crystal energy. In the Ti/$Si_{1-x}Ge_x$ system, excess Ge combines with the Si and Ge diffusing into the C54 grain boundaries from the substrate and nucleates as $Si_{1-z}Ge_z$ ($z > x$) along the grain boundaries. In the $Co/Si_{1-x}Ge_x$ system, excess Ge diffuses to the sample surface through grain boundary and surface diffusion to form Ge-enriched clusters. Once Ge is segregated out from $Co(Si_{1-y}Ge_y)$, $CoSi_2$ begins to nucleate from the CoSi.

Acknowledgements

This work is supported in part by the US Department of Energy, Division of Materials Science under contract DE-FG05-89ER45384 and by the National Science Foundation under grant DMR 9204285.

References

[1] J.M. Stork, E.J. Prinz and C.W. Magee, *IEEE Electron. Device Lett., 12* (1991) 303.
[2] P.M. Garone, V. Venkataraman and J.C. Sturm, *IEDM, 90* (1990) 383.
[3] M. Arienzo, J.H. Comfort, E.F. Crabbe, D.L. Harame, S.S. Iyer, B.S. Meyerson, G.L. Patton, J.M.C. Stork and Y.C. Sunnin, *Mater. Res. Soc. Proc., 220* (1991) 421.
[4] D.C. Houghton, J.P. Noel and N.L. Rowell, *Mater. Res. Soc. Proc., 220 299* (1992).
[5] Q.Z. Hong and J.W. Mayer, *J. Appl. Phys., 66* (1989 611)
[6] H.K. Liou, X. Wu and U. Gennser, *Appl. Phys. Lett., 60* (1992) 577.
[7] P.J. Wang, Chin-An Chang, B.S. Meyerson, J.O. Chu and M.J. Tejwani, *Mater. Res. Soc. Proc., 260* (1992) 863.
[8] A. Buxbaum, M. Eizenberg, A. Raizmann and F. Schaffler, *Mater. Res. Soc. Proc., 230* (1992) 151.

[9] V. Aubry, F. Meyer, R. Laval, C. Clerc, P. Warren and D. Dutartre, *Mater. Res. Soc. Proc., 320* (1992) 299.
[10] R.D. Thompson, K.N. Tu, J. Angillelo, S. Delage and S.S. Iyer, *J. Electrochem. Soc., 135* (1988) 3161.
[11] O. Thomas, F.M. D'Heurle, S. Delage and G. Scilla, *Appl. Surf. Sci., 38* (1989) 27.
[12] O. Thomas, F.M. d'Heurle and S. Delage, *J. Mater. Res., 5* (1990) 1453.
[13] D.B. Aldrich, Y.L. Chen, D.E. Sayers and R.J. Nemanich, *Mater. Res. Soc. Proc., 320* (1994) 305.
[14] S.P. Ashburn, M.C. Öztürk, G. Harris, D.M. Maher, D.B. Aldrich and R.J. Nemanich, *J. Appl. Phys.*, to be published.
[15] S.P. Ashburn, *Dissertation Thesis*, North Carolina State University, 1994.
[16] M.C. Ridgway, R.G. Elliman, N. Hauser, J.-M. Baribeau and T.E. Jackman, *Mater. Res. Soc. Proc., 260* (1992 857)
[17] M.C. Ridgway, M.R. Rao and J.M. Baribeau, *Mater. Res. Soc. Proc., 320* (1994) 329.
[18] G.P. Watson, D. Monroe, J-Y Cheng, E.A. Fitzgerald, Y-H Xie and R.B. Vandover, *Mater. Res. Soc. Proc., 320* (1994) 323.
[19] W-J Qi, B-Z Li, W-N Huang and Z-Q Gu, *J. Appl. Phys., 77* (1995) 1086.
[20] Z. Wang, Y.L. Chen, H. Ying, R.J. Nemanich and D.E. Sayers, *Mater. Res. Soc. Proc., 320* (1994) 397.
[21] S.P. Murarka, *Metallization: Theory and Practice for VLSI and ULSI*, Butterworth–Heinemann, Boston, MA, 1993.
[22] P. Villars and L.D. Calvert (eds.), *Pearson's Handbook of Crystallographic Data for Intermetallic Phases*, ASM International, Materials Park, OH, 1991.
[23] O. Thomas, F.M. d'Heurle, S. Delage and G. Scilla, *Appl. Surf. Sci., 38* (1989) 27–36.
[24] D.B. Aldrich, C.L. Jahncke, R.J. Nemanich and D.E. Sayers, *Mater. Res. Soc. Proc., 221* (1991) 343.
[25] D.B. Aldrich, R.J. Nemanich and D.E. Sayers, *Jpn. J. Appl. Phys., 32* (1993) 725.
[26] A. Appelbaum, R.V. Knoell and S.P. Murarka, *J. Appl. Phys., 57* (1985) 1880.
[27] G. Ottaviani, K.N. Tu, P. Psaras and C. Nobili, *J. Appl. Phys., 62* (1987) 2290.
[28] S.P. Ashburn, M.C. Öztürk, G. Harris and D.M. Maher, *J. Appl. Phys., 74* (1993) 4455.
[29] F. Wald and S.J. Michalik, *J. Less-Common Met., 24* (1971) 277.
[30] N. Boutarek and R. Madar, *Appl. Surf. Sci., 73* (1993) 209–213.
[31] D.B. Aldrich, Y.L. Chen, D.E. Sayers and R.J. Nemanich, S.P. Ashburn and M.C. Öztürk, *J. Appl. Phys.*, to be published.
[32] R. Pretorius, T.K. Marais and C.C. Theron, *Mater. Sci. Eng., 10* (1993) 1.